

# Knowledge Graph Representations to enhance Intensive Care Time-Series Predictions

**Samyak Jain**  
**Manuel Burger**  
**Gunnar Rätsch**  
**Rita Kuznetsova**

JAINSAMYAK2512@GMAIL.COM  
 MANUEL.BURGER@INF.ETHZ.CH  
 RAETSCH@INF.ETHZ.CH  
 RITA.KUZNETSOVA@INF.ETHZ.CH

*Department of Computer Science, ETH Zürich, Switzerland*

## Abstract

Intensive Care Units (ICU) require comprehensive patient data integration for enhanced clinical outcome predictions, crucial for assessing patient conditions. Recent deep learning advances have utilized patient time series data, and fusion models have incorporated unstructured clinical reports, improving predictive performance. However, integrating established medical knowledge into these models has not yet been explored. The medical domain's data, rich in structural relationships, can be harnessed through knowledge graphs derived from clinical ontologies like the Unified Medical Language System (UMLS) for better predictions. Our proposed methodology integrates this knowledge with ICU data, improving clinical decision modeling. It combines graph representations with vital signs and clinical reports, enhancing performance, especially when data is missing. Additionally, our model includes an interpretability component to understand how knowledge graph nodes affect predictions.

**Keywords:** Knowledge Graphs, Graph Neural Networks, Time-Series, Intensive Care, UMLS

appropriate modeling architectures to capture the complex interdependencies of medical data better, ultimately leading to more accurate and reliable clinical predictions. To bridge this gap, we propose a methodology that integrates these structured relationships into ICU time series predictions using knowledge graphs (KGs). Our approach, which involves jointly learning graph representations alongside time series and clinical reports, significantly enhances model performance, particularly in cases with missing data. The main contributions are as follows:

- **Usage of prior medical knowledge:** We construct KGs using the UMLS database, demonstrating that the incorporation of a strong structural prior into our model leads to enhanced performance.
- **Performance under Missing Data:** Graph structure-based methods have shown strong performance in scenarios with missing data (Zhang et al., 2021). Building on this, our approach diverges by jointly learning representations across various modalities, which further improves performance in situations with missing data.
- **Interpretability:** In the medical domain, machine learning systems must be not only reliable but also interpretable and explainable. We identify the most influential KG nodes and examine their impact on the model's predictions.

Experimental results from the MIMIC-III Benchmark tasks (Johnson et al., 2016b; Harutyunyan et al., 2019) show that the use of prior knowledge not only enhances predictive performance but also yields better results with increasing amounts of missing data. Additionally, our interpretability analysis highlights the most predictive medical concepts within our knowledge graph.

## 1. Introduction

Recently, researchers have investigated the use of multimodal data types (Khadanga et al., 2019; Husmann et al., 2022), including patient time series and unstructured clinical reports, for predictive tasks in Intensive Care Units (ICU) (Harutyunyan et al., 2019; Yèche et al., 2021). However, these approaches often overlook the rich structured relationships inherent in the medical domain, such as those in clinical ontologies like the Unified Medical Language System (UMLS) (Bodenreider, 2004). These ontologies exhibit a structural prior, which can be exploited by ap-

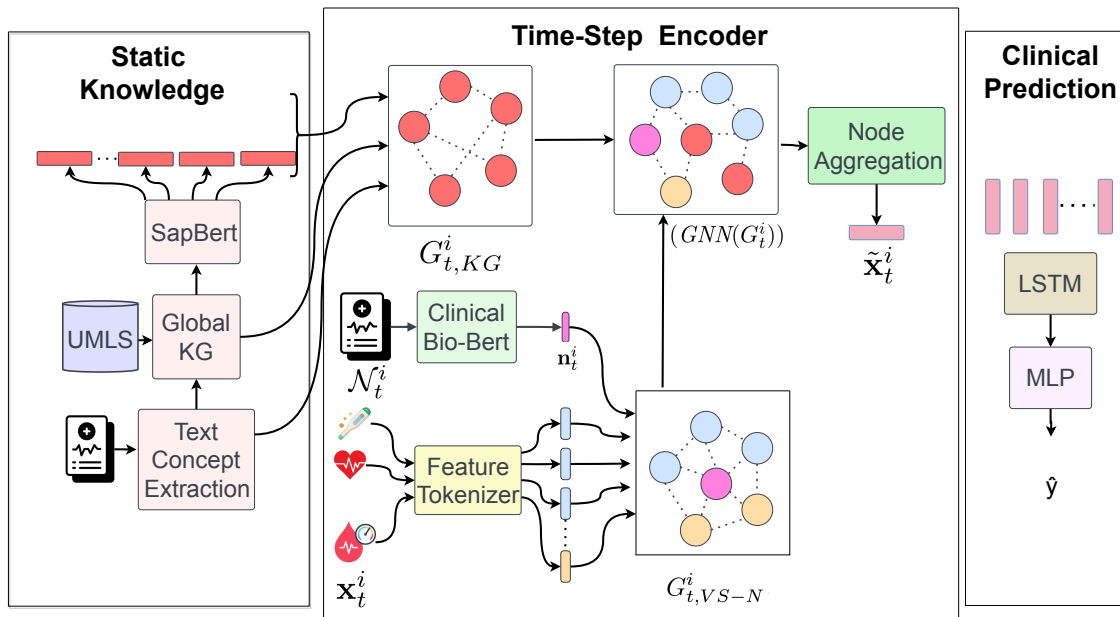


Figure 1: Architecture Diagram: We extract *Static Knowledge* (Sec. 3.1), we compute a rich multi-modal *time-step embedding* including structured knowledge (Sec. 3.2) and then perform clinical prediction tasks (Sec. 3.3).

## 2. Related Work

In the subsequent sections, we discuss related work on multi-modal approaches, encompassing Large Language Models and the use of prior knowledge through KGs, in the context of ICU data.

**Multi-Modality** Prior research in learning representations from multimodal data has explored a wide range of approaches. These approaches include: combining sequence models with convolutional feature extractors to process clinical notes (Khadanga et al., 2019); integrating sequence models with BERT (Devlin et al., 2018; Deznabi et al., 2021); leveraging Named Entity Recognition models in conjunction with word and document embeddings to capture structured information (Bardak and Tan, 2021) and employing cross-modal transformers to effectively model relationships between different modalities (Husmann et al., 2022).

**Graph Approaches** Recent studies have explored the utilization of relational structures among different variables through the application of Graph Neural Networks (GNNs). Zhang et al. (2021) introduced a model that leverages these relational struc-

tures. Another approach (Zhang et al., 2022) incorporates a patient correlation graph fusion model. However, these works do not incorporate prior medical knowledge from diverse sources and vocabularies and are also not suitable for online prediction tasks. Alternatively, there is a separate line of research that utilizes such knowledge in the form of knowledge graphs to enhance predictions. Notably, these knowledge-enhanced approaches are primarily focused on tasks related to subsequent hospital admissions (Burger et al., 2023; Jiang et al., 2023) or non-sequence tasks (Roy and Pan, 2021; Chandak et al., 2023) rather than multi-variate ICU time series analysis.

**Language Models** Finally, language models have been proposed to solve clinical tasks (Yasunaga et al., 2022; Nori et al., 2023). However, such models cannot natively handle the diverse set of numerical and categorical clinical variables in the form of a multi-variate time series to perform prediction tasks in an intensive care setting.

**Our Work** In this study, we leverage prior medical knowledge, clinical notes, and graph structures to enhance multi-variate ICU time series models. Our

approach also explores how the combination of these modalities can mitigate challenges in scenarios with missing data. These models are designed with a specific focus on ICU prediction tasks while remaining suitable for online predictions (contiguous predictions at every time step).

### 3. Methodology

In this section, we formally introduce our method and how we incorporate prior knowledge into the time-series model. We consider a dataset  $\mathcal{D}$  of multiple patient time series. The time-series of patient  $i$  of length  $T$  is  $\mathbf{X}^i = [\mathbf{x}_1, \mathbf{x}_2, \dots, \mathbf{x}_T]$  and consists of time-steps  $\mathbf{x}_t^i = [x_{t,1}, x_{t,2}, \dots, x_{t,n_{VS}}] \in \mathbb{R}^{n_{VS}}$ , where we observe  $n_{VS}$  vital signs measurements. Additionally, let  $\mathcal{N}_t^i$  be the set of clinical notes available at time  $t$  for patient  $i$  (details on clinical notes in App. A.3). We obtain the aggregated representation of all clinical notes at each time-step  $\mathbf{n}_t^i = \text{BERT}(\mathcal{N}_t^i) \in \mathbb{R}^d$  using a pre-trained Clinical Bio-Bert model (Alsentzer et al., 2019).

#### 3.1. Static Knowledge

We build a concept extraction pipeline using QuickUMLS (Soldaini and Goharian, 2016) to obtain the set of medical concepts found in clinical notes  $V_t^i = \text{QuickUMLS}(\mathcal{N}_t^i)$ . We then build a global medical knowledge graph  $G = (V, E)$  as follows in Eqn. 1:

$$V = \bigcup_{i,t \in \mathcal{D} \times T} V_t^i, \quad (1)$$

$$E = \{\{u, v\} \mid \forall \{u, v\} \in \text{UMLS} \wedge u, v \in V\}$$

with nodes  $V$  and (undirected) edges (as node sets  $\{u, v\}$ ) from the UMLS database  $E$ . We use the SapBERT model (Gu et al., 2020) on the node descriptors available in UMLS to obtain node representations. Figure 1 (left) demonstrates the process.

#### 3.2. Time-Step Encoder

In this section, we describe how to obtain a rich step embedding using different modalities for each patient  $i$  at each time-step  $t$ .  $\mathbf{x}_t^i \in \mathbb{R}^{n_{VS}}$  is given as input to the Feature Tokenizer (FT) module (Gorishniy et al., 2021) to convert each of the  $n_{VS}$  measurements into an embedding. We concatenate the clinical note representation  $\mathbf{n}_t^i$  and obtain for each time-step the vital signs and text (clinical notes) matrix:

$$\mathbf{X}_{t,VS-N}^i = [\text{FT}(\mathbf{x}_t^i); \mathbf{n}_t^i] \in \mathbb{R}^{(n_{VS}+1) \times d} \quad (2)$$

We then build the vital signs and text (clinical notes) graph:

$$G_{t,VS-N}^i = (\mathbf{X}_{t,VS-N}^i, E_{VS-N}) \quad (3)$$

where  $E_{VS-N}$  corresponds to edge connectivity based on prior knowledge (e.g. organ system assignments of vitals) or full connectivity amongst vitals. The text node  $\mathbf{n}_t^i$  is connected to all vitals. To incorporate prior knowledge a subgraph  $G_{t,KG}^i$  is formed by querying the global graph  $G$  using the extracted concepts  $V_t^i$  at the timepoint  $t$  for patient  $i$ .

$$E_{t,KG}^i = \{\{u, v\} \mid \forall \{u, v\} \in E \wedge u, v \in V_t^i\} \quad (4)$$

$$G_{t,KG}^i = (\mathbf{X}_{t,KG}^i, E_{t,KG}^i) \quad (5)$$

where  $\mathbf{X}_{t,KG}^i$  are the SapBERT node embeddings and  $E_{t,KG}^i$  are edges from the global knowledge graph  $G$  (see Sec. 3.1). We then join  $G_{t,VS-N}^i$  and  $G_{t,KG}^i$  by adding undirected edges from all nodes in  $G_{t,VS-N}^i$  to all nodes in  $G_{t,KG}^i$  to obtain the final dynamic time-step graph  $G_t^i$ :

$$\bar{E}_t^i = \{\{u, v\} \mid \forall u \in G_{t,VS-N}^i, \forall v \in G_{t,KG}^i\} \quad (6)$$

$$E_t^i = \bar{E}_t^i \cup E_{t,KG}^i \cup E_{VS-N} \quad (7)$$

$$G_t^i = (\mathbf{X}_{t,VS-N}^i \cup \mathbf{X}_{t,KG}^i, E_t^i) \quad (8)$$

Information is exchanged among the nodes of each dynamic graph  $G_t^i$  using GNN layers and finally, all nodes are aggregated to form a rich *step embedding*  $\tilde{\mathbf{x}}_t^i = \text{AGG}(\text{GNN}(G_t^i)) \in \mathbb{R}^d$ . For AGG we use non-parametric aggregation functions such as *sum*, *mean*, or *max*. Figure 1 (middle) demonstrates the process.

#### 3.3. Clinical Prediction

Based on the previous Section 3.2 we obtain a *step embedding*  $\tilde{\mathbf{x}}_t^i$  at each time point. The sequence of time step embeddings is processed by a sequence model (such as LSTM (Hochreiter and Schmidhuber, 1997)) and followed by a Multi-Layered Perceptron (MLP) that uses the hidden state(s) of the LSTM network to generate the final prediction.

## 4. Experimental Setup

**Data Processing** We perform our experiments on the MIMIC-III dataset (Johnson et al., 2016b). To avoid data leakage we remove all discharge summary notes and mask out the last available notes as they often contain explicit mortality terms (Husmann et al., 2022). For more details, we refer to the App. A.

Table 1: Model Performance Comparison on MIMIC-III Benchmark tasks (Harutyunyan et al., 2019).

Method	Mortality		Decompensation		Phenotyping	
	<i>AuPRC</i>	<i>AuROC</i>	<i>AuPRC</i>	<i>AuROC</i>	<i>macro-AUC</i>	<i>micro-AUC</i>
Harutyunyan et al. (2019)	50.1 ± 1.3	86.1 ± 0.3	34.1 ± 0.5	90.7 ± 0.2	77.6 ± 0.4	82.5 ± 0.3
Khadanga et al. (2019)	52.5 ± 1.3	86.5 ± 0.4	34.5 ± 0.7	90.7 ± 0.7	-	-
Husmann et al. (2022)	52.7 ± 1.0	87.1 ± 0.6	39.7 ± 0.6	92.2 ± 0.2	82.6 ± 0.1	86.1 ± 0.1
Yang et al. (2021)	56.2 ± na	85.7 ± na	-	-	-	-
Zhang et al. (2021)	44.6 ± 2.1	83.7 ± 0.5	-	-	-	-
<i>Ours</i>	<b>58.7 ± 0.6</b>	<b>89.3 ± 0.1</b>	<b>47.2 ± 1.0</b>	<b>94.2 ± 0.3</b>	<b>84.6 ± 0.1</b>	<b>87.9 ± 0.1</b>

**Tasks** We analyze the performance of the model on established benchmark tasks (Harutyunyan et al., 2019). We focus on 3 clinical prediction tasks. 1) In-hospital mortality is a binary prediction task using data from the first 48 hours of patient stay. 2) Decompensation is an hourly online prediction task with a binary label stating whether a patient will die in the next 24 hours or not. 3) Phenotyping uses the entire time series of a patient stay and classifies it into 25 acute care conditions.

**Architecture** Different hyperparameters of our architecture were selected using a grid/random search approach to optimize validation set performance on the mortality task. Details can be found in App. B.

## 5. Results

We compare the performance of the proposed solution with other existing multi-modal fusion methods. Table 1 shows the comparison and it is evident that we outperform other methods. Harutyunyan et al. (2019) provided initial benchmark baselines using different time-series architectures on vital signs data. Khadanga et al. (2019); Yang et al. (2021) propose multi-modal fusion architectures with separate encoders for each modality and Husmann et al. (2022) benchmark a multi-modal transformer with cross-attention across the modalities at every layer. Finally, Zhang et al. (2021) introduced a graph-structured model with increased robustness on missing data to process irregularly sampled vital signs time series. Our results highlight the benefits of pairing multi-modal fusion with prior knowledge using graph-structured time-step embeddings.

**Performance under Missing Data** We ascertain the model’s performance under missing data by randomly masking vital signs data of the test set (Zhang et al., 2021). Figure 2 shows how the performance

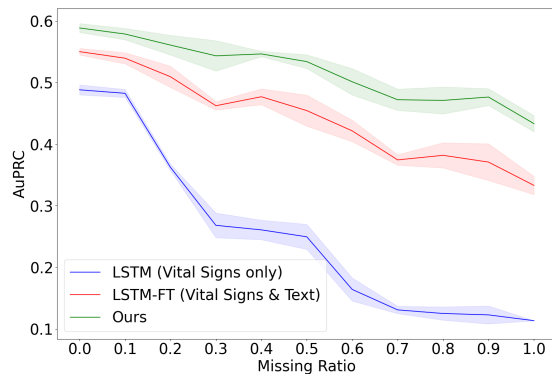


Figure 2: Performance under Missing Data on the Mortality prediction task after 48 hours of patient stay. Shaded areas indicate standard deviations.

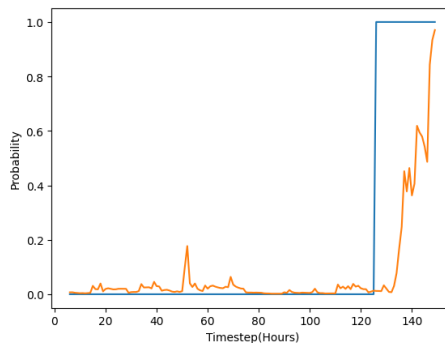


Figure 3: Decompensation Analysis of Patient ID 11486: *orange* line shows the model’s predicted probability for the binary decompensation label and the *blue* line depicts the ground-truth label

of different methods varies with different missing ratios. A missing ratio refers to the amount of masking e.g. *missing ratio* = 0.5 implies 50% of the vital

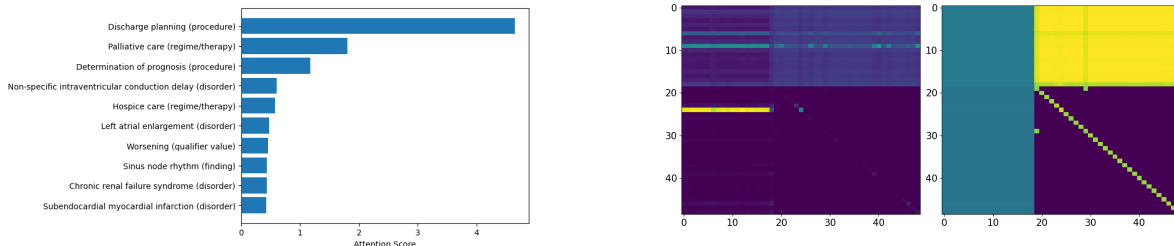


Figure 4: Decompenation Analysis of Patient ID 11486 : (left) Attention Scores of top 10 KG nodes aggregated the entire time-series; (right) Attention Score HeatMap(s) at timestep 138 of the two employed GNN layers. Lower indices correspond to vital signs nodes from  $G_{t,VS-N}^i$  and higher indices correspond to nodes from the time-point specific (sub-)knowledge graph  $G_{t,KG}^i$ .

signs data is masked. We observe increased robustness under missing data in case of multi-modal inputs (e.g. including text, red curve) and an additional improvement under our proposed rich, multi-modal, knowledge-enhanced, and graph-structured step embedding (green curve).

We do note, that models considering multiple modalities such as text and/or knowledge graph concepts perform well even under high amounts of missing vital signs data. Inspection of relevant clinical notes reveals explicit discussion of hospital staff on discharge planning or certain disorders, which are highly indicative for tasks such as *mortality* or *decompensation*. This behavior is further emphasized in our proposed method by explicitly extracting related medical concepts and not only embedding entire pieces of text. In the following paragraph, we show strong attention of the model on task-related knowledge graph nodes such as *palliative care*.

**Interpretability** Leveraging a Graph Attention Network (GAT) by Veličković et al. (2017), we compute attention scores across KG nodes, highlighting the significance of procedural (e.g., discharge planning), therapeutic (e.g., palliative care and hospice care), and disorder-related nodes (see Figure 4 (left)).

We then conduct an interpretability analysis to investigate the model’s predictions, emphasizing temporal dynamics as illustrated in Figure 3. We can see a strong increase in the predicted probability of decompensation around time-point 140. A focused examination of the time-step graph  $G_t^i$  at time-step 138 provides insight into notable changes in the predicted probability of decompensation. Figure 4 (right) shows the heatmaps after the first and second

GNN layers at time step 138. They depict the attention matrix formed using different nodes of the time-step graph  $G_t^i$ , where lower indices correspond to nodes from  $G_{t,VS-N}^i$  and higher indices correspond to nodes from  $G_{t,KG}^i$  (Sec. 3.2). From the left heatmap (i.e. the first GNN layer) the 24th entry has particularly high attention. The specific node is the knowledge graph concept corresponding to *palliative care*. As *palliative care* is specialized care for people with serious illnesses, the model appropriately learned its correlation with the decompensation target.

We conclude that the extraction of prior medical knowledge aids interpretability at a detailed level of individual time steps. Further, we would like to underline the relevance of extracting and structuring model inputs based on prior knowledge concepts to provide more precise signals to our learning algorithms.

## 6. Conclusion

We investigated the impact of incorporating Knowledge Graphs, derived from prior medical knowledge, on ICU time series clinical prediction tasks. We introduced a novel method for extracting and utilizing this knowledge in ICU predictions. Our findings highlight the effectiveness of graph-structured architectures with prior knowledge, particularly in scenarios with increasing missing data, which is a common challenge in clinical data applications. Furthermore, we emphasize the significance of discretely extracted prior knowledge concepts, which enhance both interpretability and learning signals.

## Acknowledgments

This project was supported by grant #2022-278 of the Strategic Focus Area “Personalized Health and Related Technologies (PHRT)” of the ETH Domain (Swiss Federal Institutes of Technology).

## References

- Emily Alsentzer, John R Murphy, Willie Boag, Wei-Hung Weng, Di Jin, Tristan Naumann, and Matthew McDermott. Publicly available clinical bert embeddings. *arXiv preprint arXiv:1904.03323*, 2019.
- Batuhan Bardak and Mehmet Tan. Improving clinical outcome predictions using convolution over medical entities with multimodal learning. *Artificial Intelligence in Medicine*, 117:102112, 2021.
- Olivier Bodenreider. The unified medical language system (umls): integrating biomedical terminology. *Nucleic acids research*, 32(suppl.1):D267–D270, 2004.
- Manuel Burger, Gunnar Rätsch, and Rita Kuznetsova. Multi-modal graph learning over umls knowledge graphs. *arXiv preprint arXiv:2307.04461*, 2023.
- Payal Chandak, Kexin Huang, and Marinka Zitnik. Building a knowledge graph to enable precision medicine. *Scientific Data*, 10(1):67, 2023.
- Jacob Devlin, Ming-Wei Chang, Kenton Lee, and Kristina Toutanova. Bert: Pre-training of deep bidirectional transformers for language understanding. *arXiv preprint arXiv:1810.04805*, 2018.
- Iman Deznabi, Mohit Iyyer, and Madalina Fiterau. Predicting in-hospital mortality by combining clinical notes with time-series data. In *Findings of the association for computational linguistics: ACL-IJCNLP 2021*, pages 4026–4031, 2021.
- Yury Gorishniy, Ivan Rubachev, Valentin Khrukov, and Artem Babenko. Revisiting deep learning models for tabular data. *Advances in Neural Information Processing Systems*, 34:18932–18943, 2021.
- Yu Gu, Robert Timm, Hao Cheng, Michael Lucas, Naoto Usuyama, Xiaodong Liu, Tristan Naumann, Jianfeng Gao, and Hoifung Poon. Domain-specific language model pretraining for biomedical natural language processing, 2020.
- Hrayr Harutyunyan, Hrant Khachatrian, David C Kale, Greg Ver Steeg, and Aram Galstyan. Multi-task learning and benchmarking with clinical time series data. *Scientific data*, 6(1):96, 2019.
- Sepp Hochreiter and Jürgen Schmidhuber. Long short-term memory. *Neural Comput.*, 9(8):1735–1780, nov 1997. ISSN 0899-7667. doi: 10.1162/neco.1997.9.8.1735. URL <https://doi.org/10.1162/neco.1997.9.8.1735>.
- Severin Husmann, Hugo Yèche, Gunnar Rätsch, and Rita Kuznetsova. On the importance of clinical notes in multi-modal learning for ehr data. *arXiv preprint arXiv:2212.03044*, 2022.
- Pengcheng Jiang, Cao Xiao, Adam Cross, and Jimeng Sun. Graphcare: Enhancing healthcare predictions with open-world personalized knowledge graphs. *arXiv preprint arXiv:2305.12788*, 2023.
- Alistair EW Johnson, Tom J Pollard, Lu Shen, Liwei H Lehman, Mengling Feng, Mohammad Ghassemi, Benjamin Moody, Peter Szolovits, Leo Anthony Celi, and Roger G Mark. Mimic-iii, a freely accessible critical care database. *Scientific data*, 3(1):1–9, 2016a.
- Alistair EW Johnson, Tom J Pollard, Lu Shen, Liwei H Lehman, Mengling Feng, Mohammad Ghassemi, Benjamin Moody, Peter Szolovits, Leo Anthony Celi, and Roger G Mark. Data descriptor: Mimic-iii, a freely accessible critical care database (2016), 2016b.
- Swaraj Khadanga, Karan Aggarwal, Shafiq Joty, and Jaideep Srivastava. Using clinical notes with time series data for icu management. *arXiv preprint arXiv:1909.09702*, 2019.
- Diederik P Kingma and Jimmy Ba. Adam: A method for stochastic optimization. *arXiv preprint arXiv:1412.6980*, 2014.
- Harsha Nori, Nicholas King, Scott Mayer McKinney, Dean Carignan, and Eric Horvitz. Capabilities of gpt-4 on medical challenge problems, 2023.
- Arpita Roy and Shimei Pan. Incorporating medical knowledge in bert for clinical relation extraction. In *Proceedings of the 2021 conference on empirical methods in natural language processing*, pages 5357–5366, 2021.

Luca Soldaini and Nazli Goharian. Quickumls: a fast, unsupervised approach for medical concept extraction. In *MedIR workshop, sigir*, pages 1–4, 2016.

Umeicon, Good Ware, juicy\_fish, and Vector Squad. Flaticon, 2023. URL <https://www.flaticon.com/>.

Petar Veličković, Guillem Cucurull, Arantxa Casanova, Adriana Romero, Pietro Lio, and Yoshua Bengio. Graph attention networks. *arXiv preprint arXiv:1710.10903*, 2017.

Haiyang Yang, Li Kuang, and FengQiang Xia. Multimodal temporal-clinical note network for mortality prediction. *Journal of Biomedical Semantics*, 12(1):1–14, 2021.

Michihiro Yasunaga, Antoine Bosselut, Hongyu Ren, Xikun Zhang, Christopher D Manning, Percy Liang, and Jure Leskovec. Deep bidirectional language-knowledge graph pretraining, 2022.

Hugo Yèche, Rita Kuznetsova, Marc Zimmermann, Matthias Hüser, Xinrui Lyu, Martin Faloutsos, and Gunnar Rätsch. Hirid-icu-benchmark—a comprehensive machine learning benchmark on high-resolution icu data. *arXiv preprint arXiv:2111.08536*, 2021.

Xiang Zhang, Marko Zeman, Theodoros Tsiligkaridis, and Marinka Zitnik. Graph-guided network for irregularly sampled multivariate time series. *arXiv preprint arXiv:2110.05357*, 2021.

Ying Zhang, Baohang Zhou, Kehui Song, Xuhui Sui, Guoqing Zhao, Ning Jiang, and Xiaojie Yuan. Pm2f2n: Patient multi-view multi-modal feature fusion networks for clinical outcome prediction. In *Findings of the Association for Computational Linguistics: EMNLP 2022*, pages 1985–1994, 2022.

## Appendix A. Dataset

### A.1. Pre-processing

For the vital signs data, we follow the preprocessing steps outlined in Harutyunyan et al. (2019). For clinical text notes, we follow the preprocessing steps outlined in Husmann et al. (2022). Essentially for all text notes that do not have CHARTTIME information, we set their CHARTTIME to the end of the respective CHARTDATE, remove all discharge summary notes, and then mask the last text note available. Post the filtering we exclude all patients without any text note similar to Khadanga et al. (2019).

### A.2. Task Statistics

We provide the statistics for the test set on mortality and decompensation tasks.

Table 2: Decompensation

Label	# labels
0	511900
1	9403
Total	521303

Table 3: Mortality

Label	# labels
0	2853
1	365
Total	3218

### A.3. Clinical Notes

We provide some details on the clinical notes published in the MIMIC-III Johnson et al. (2016a) dataset in the NOTEEVENTS table.

In total, there are about 2 million individual text notes of 15 categories (e.g. *Discharge summary, Radiology, Nursing, Physician, Nutrition, General, Pharmacy*, etc.). The median length of such a note is at 1,090 characters and we observe a median of about 14 individual notes per patient (with 7 at the first quartile and 30 at the third quartile).

Each note is associated with a specific timestamp (CHARTDATE and CHARTTIME) during a single admission (HADM\_ID) of a given patient (SUBJECT\_ID). However, for a given patient admission we do not observe a note at every single time point on our resampled grid used during training. Some time points might have no clinical note associated with them, whereas others might have multiple, and they thus build an irregularly sampled time series of textual descriptions of the patient state. As such the set of clinical notes  $\mathcal{N}_t^i$  at time  $t$  given patient  $i$  might be empty. In that case, the representation  $\mathbf{n}_t^i$  is a 0-vector.

## Appendix B. Hyperparameters

We extract knowledge subgraphs  $G_{t,KG}^i$  with a maximum of 30 nodes, use a 2-layered GNN, and set all latent space embedding dimensions to 64. We rely on the Adam optimizer (Kingma and Ba, 2014) to train all the models with a learning rate of  $1e^{-4}$ . Details of other hyperparameters searched can be found in table 4

Table 4: Hyperparameters for Experiments

Parameters	Values
Batch Size	(8, 16, 32, 64)
Embedding Size	(64)
GNN Depth	(0,1,2)
Graph Convolution	(GCN, GAT, <b>GraphSAGE</b> )
Learning rate	( <b>1e-4</b> , 1e-3)
Hidden Size (LSTM)	(100)
# KG Nodes	(0, 6, 18, <b>30</b> , 42, 54, 66, 78)
Nodes Aggregation	( <b>sum</b> , mean, max)
Epochs	(20, 40)

Parameters in bold indicate the choice that performed best. Batch size was varied across tasks so that the data could fit in the GPU memory. 20 epochs sufficed for mortality and decompensation tasks and 40 was used for phenotyping.

## Appendix C. Ablation Studies

In this section, we show how the incremental addition of model components impacts performance.

Table 5 shows the performance variation on the mortality task when different model components/features are added incrementally. As seen in the case of Vital Signs-only data addition of the feature tokenizer module improves the performance, however further addition of the graph conv layer does not help much. With Vital Signs and Text data combined one can see a significant boost in performance due to the addition of the FT module, the addition of the graph conv layer does not improve overall performance. Finally, incorporating prior medical knowledge in the form of KG also helps and enhances performance.



Table 5: Mortality Performance Study under Different Model Components

Model Component	AuPRC	AuROC
LSTM (Vital Signs only)	49.5 +/- 0.6	85.6 +/- 0.3
LSTM-FT (Vital Signs only)	51.2 +/- 0.1	85.9 +/- 0.2
LSTM-FT-GNN (Vital Signs only)	51.2 +/- 0.5	85.6 +/- 0.1
LSTM (Vital Signs & Text)	52.8 +/- 1.0	87.3 +/- 0.3
LSTM-FT (Vital Signs & Text)	55.2 +/- 0.9	87.7 +/- 0.1
LSTM-FT-GNN (Vital Signs & Text)	55.6 +/- 0.5	88.1 +/- 0.1
LSTM-FT-GNN (Vital Signs & Text & KG)	<b>58.9 +/- 0.4</b>	<b>88.9 +/- 0.1</b>

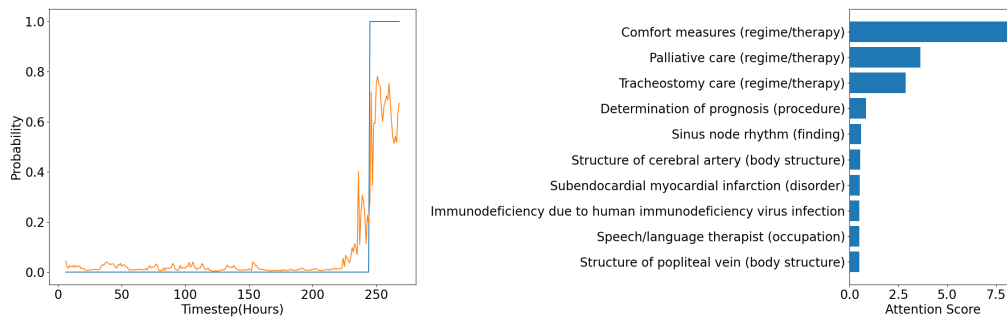


Figure 5: Decompenation Analysis of Patient Id - 16236 : (left) *orange* line shows the model's prediction and *blue* line depicts the ground-truth label; (right) Attention Scores of KG nodes

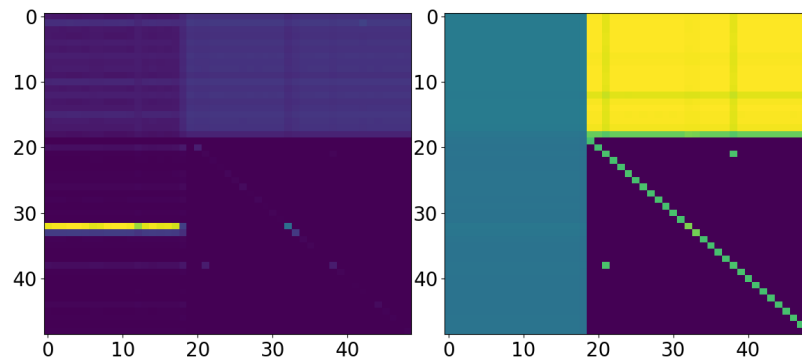


Figure 6: HeatMap(s) at timestep 235

## Appendix D. Interpretability Results

### D.1. Analysis of Patient ID: 16236 (3rd Episode)

Figure 5 gives another illustrative example to show the model's behavior on the decompenation task. In this example, different medical concepts related to therapies like *Comfort Measures*, *Palliative Care*,

and *Tracheostomy Care* form the most significant knowledge graph nodes. Figure 5 shows heatmaps at timestep 235. On the left heatmap, the 32nd entry has high attention and on inspection, it was the *Palliative care* knowledge graph node similar to the previous example.

**D.2. Analysis of Patient ID: 18129 (1st Episode)**

Figure 7 gives another illustrative example. In this case, the prognosis bad node has an extremely high attention score. A bad prognosis means that the patient has very little chance of recovery. From the left heatmap of figure 8, the 27th entry has high attention, and on inspection, to no surprise, the node was prognosis bad.

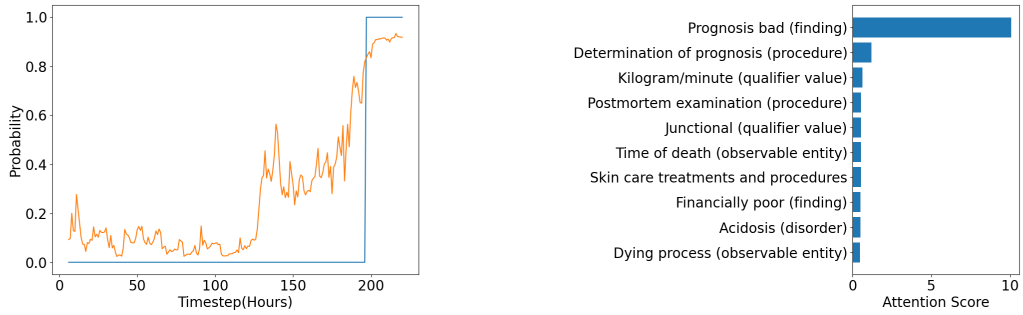


Figure 7: Decompenation Analysis of Patient Id - 18129 : (left) *orange* line shows the model's prediction and *blue* line depicts the ground-truth label; (right) Attention Scores of KG nodes

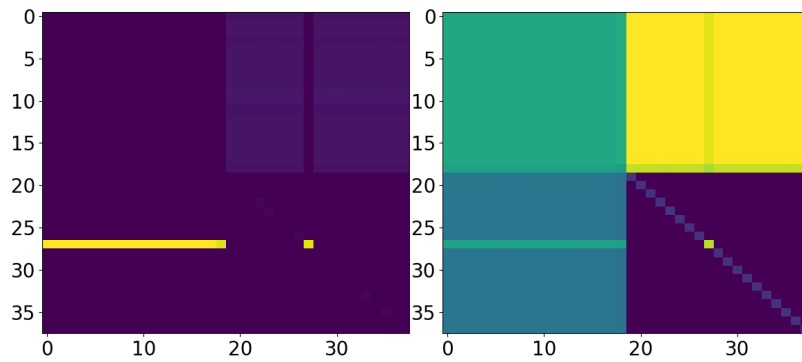


Figure 8: HeatMap(s) at timestep 148